

Solid Lipid Nanoparticles for the Co-Delivery of Nilotinib and Rutin: A Comprehensive Strategy to Enhance Efficacy and Reduce Toxicity in Cancer Treatment

Santhi M¹, Divyadharshini S^{2*}

¹P.G Student, Department of Pharmaceutics, J. K. K. Nattraja college of pharmacy, Kumarapalayam-638613, Namakkal dt, Tamil Nadu, India

²Assistant Professor, Department of Pharmaceutics, J. K. K. Nattraja college of pharmacy, Kumarapalayam-638613, Namakkal dt, Tamil Nadu, India

DOI: <https://doi.org/10.36348/sjbr.2026.v11i02.001>

| Received: 03.12.2025 | Accepted: 31.01.2026 | Published: 09.02.2026

*Corresponding author: Divyadharshini S

Assistant Professor, Department of Pharmaceutics, J. K. K. Nattraja college of pharmacy, Kumarapalayam-638613, Namakkal dt, Tamil Nadu, India

Abstract

Cancer remains one of the leading causes of morbidity and mortality worldwide, necessitating the development of advanced therapeutic strategies with improved efficacy and reduced toxicity. Conventional cancer treatments are often limited by poor drug solubility, non-specific distribution, systemic side effects, and the development of drug resistance. Targeted drug delivery systems, particularly nanotechnology-based approaches, have emerged as promising solutions to overcome these challenges. Solid Lipid Nanoparticles (SLNs) are biocompatible and biodegradable carriers capable of enhancing drug stability, bioavailability, controlled release, and targeted delivery. Nilotinib, a second-generation BCR-ABL tyrosine kinase inhibitor, is widely used in the treatment of chronic myeloid leukemia; however, its clinical application is constrained by limited bioavailability and adverse effects. Rutin, a natural bioflavonoid, exhibits potent antioxidant, anti-inflammatory, anti-angiogenic, and pro-apoptotic properties, making it a valuable adjunct in cancer therapy. The co-encapsulation of Nilotinib and Rutin into SLNs offers a synergistic therapeutic approach by enhancing solubility, improving cellular uptake, reducing systemic toxicity, and overcoming multidrug resistance. This project focuses on the formulation and application of Nilotinib and Rutin-loaded SLNs as an innovative strategy for enhanced cancer treatment. The SLN-based delivery system holds significant potential for improving therapeutic outcomes and advancing personalized cancer therapy.

Keywords: Cancer, Solid Lipid Nanoparticles, Nilotinib, Rutin, Targeted Drug Delivery.

Copyright © 2026 The Author(s): This is an open-access article distributed under the terms of the Creative Commons Attribution 4.0 International License (CC BY-NC 4.0) which permits unrestricted use, distribution, and reproduction in any medium for non-commercial use provided the original author and source are credited.

1. INTRODUCTION

Cancer is a complex group of diseases characterized by the uncontrolled growth and proliferation of abnormal cells resulting from genetic and epigenetic alterations. These changes disrupt normal cell cycle regulation and arise due to environmental exposures such as tobacco smoke, radiation, chemical carcinogens, infections, lifestyle factors, or inherited genetic predisposition [1]. Under normal physiological conditions, cell growth and division are tightly regulated by signaling pathways involving cyclins, cyclin-dependent kinases, and tumor suppressor proteins, ensuring tissue homeostasis [2].

One of the fundamental hallmarks of cancer is uncontrolled cell proliferation, which occurs when regulatory checkpoints of the cell cycle are bypassed. Mutations in oncogenes such as *Ras* or loss of tumor

suppressor genes like *p53* result in continuous cell division, leading to tumor formation and progression [3]. Another key feature of cancer is resistance to apoptosis, the programmed cell death mechanism that eliminates damaged or unnecessary cells. Cancer cells evade apoptosis through mutations in the *TP53* gene, overexpression of anti-apoptotic proteins such as Bcl-2, or defects in death receptor signaling pathways, allowing survival and accumulation of abnormal cells [4].

The ability of cancer cells to invade surrounding tissues and metastasize to distant organs defines malignancy and is the leading cause of cancer-related mortality.

Metastasis involves multiple steps including local invasion, intravasation into blood or lymphatic vessels, survival in circulation, extravasation, and

colonization at secondary sites [5]. This process is facilitated by enzymes such as matrix metalloproteinases and is driven by genetic adaptations that enhance cell motility and survival in foreign microenvironments. It is important to note that cancer is not contagious and does not spread between individuals; it propagates only within the body through metastatic mechanisms [6].

Early and accurate diagnosis is critical for effective cancer management. Diagnostic approaches include physical examination, laboratory investigations (blood and urine tests), imaging techniques such as X-ray, CT, MRI, PET, and ultrasound, as well as endoscopic procedures and biopsy, which remains the gold standard for definitive diagnosis. Advances in genetic testing and screening tools such as mammography, Pap smears, and low-dose CT scans have significantly improved early detection and personalized treatment planning [7].

The evolution of cancer treatment has progressed remarkably from ancient surgical excision and herbal remedies to modern multimodal therapies. The 19th century introduced cryotherapy, radical surgical procedures, and radiation therapy following the discovery of X-rays [8, 9]. The 20th century witnessed the advent of chemotherapy with agents like mustine and methotrexate, followed by the development of targeted therapies and immunotherapy, which revolutionized cancer treatment by improving specificity and reducing systemic toxicity (10). In the 21st century, advancements in biotechnology have enabled personalized medicine, gene-based therapies, CAR-T cell therapy, anti-tumor vaccines, and monoclonal antibodies, significantly improving patient outcomes [11, 12].

From an epidemiological perspective, cancer remains a major global health burden. In 2020, over 19 million new cancer cases and approximately 10 million deaths were reported worldwide. In India alone, nearly 2.5 million individuals are living with cancer, with breast, cervical, oral, and lung cancers being most prevalent [13–15]. Lifestyle factors such as tobacco use, alcohol consumption, poor diet, obesity, environmental pollution, and infections like HPV and hepatitis viruses significantly contribute to cancer incidence and prevalence [16, 17].

Among modern therapeutic strategies, targeted drug delivery systems have gained immense importance. Nilotinib, a second-generation BCR-ABL tyrosine kinase inhibitor, has transformed the treatment of Philadelphia chromosome-positive chronic myeloid leukemia by selectively inhibiting malignant cell proliferation while minimizing damage to normal cells [18]. However, its clinical use is limited by poor bioavailability and systemic side effects. Similarly, Rutin, a naturally occurring bioflavonoid, exhibits potent antioxidant, anti-inflammatory, anti-angiogenic, and pro-apoptotic properties, making it a promising adjunct

in cancer therapy [20].

To overcome limitations of conventional therapy, Solid Lipid Nanoparticles (SLNs) have emerged as a novel drug delivery platform. SLNs are submicron-sized (10–1000 nm), biocompatible carriers composed of solid lipids stabilized by surfactants. They enhance drug solubility, stability, controlled release, and targeted delivery while reducing systemic toxicity (24,25). Co-delivery of Nilotinib and Rutin via SLNs offers a synergistic approach by improving bioavailability, overcoming multidrug resistance, enhancing therapeutic efficacy, and minimizing adverse effects [19–23].

Thus, SLN-based combination therapy represents a promising and innovative strategy in modern cancer management, paving the way for advanced nanomedicine and personalized treatment approaches.

2. AIM AND OBJECTIVE

2.1 Aim of the Work

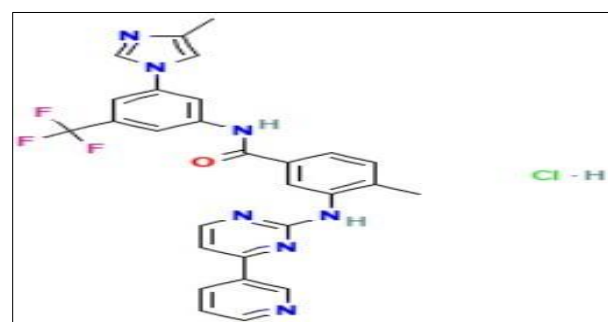
The aim of this study is to develop and characterize a SLN system for the co-delivery of Nilotinib and Rutin to enhance their therapeutic efficacy against cancer.

2.2 Objective of the Work

- To formulate and characterize Nilotinib and Rutin co-loaded SLNs, including particle size, zeta potential, encapsulation efficiency, and surface morphology.
- To investigate the *in vitro* release behaviour and determine the release kinetics of Nilotinib and Rutin from the developed SLNs.
- To conduct *in vitro* cell line studies to analyze the anticancer activity of Nilotinib, Rutin, and the Nilotinib-Rutin co-loaded SLNs

3. DRUG PROFILE

3.1 Nilotinib Hydrochloride



Generic Name: Nilotinib Hydrochloride

Synonym: AMN107

Molecular Formula: C₂₈H₂₂F₃N₇O

Molecular Weight: 529.52 g/mol

Melting Point: 231–240°C

Description: Nilotinib Hydrochloride is a white to yellowish crystalline powder.

Solubility: Poorly soluble in water (<0.1 mg/mL); freely soluble in DMSO (up to 6 mg/mL).

Category: Antineoplastic agent – BCR-ABL Tyrosine Kinase Inhibitor.

Pharmacokinetics

- Absorption:** Rapid absorption; peak plasma concentration in ~3 hours
- Metabolism:** Extensively metabolized in the liver by CYP3A4
- Excretion:** Predominantly excreted via feces (~93%)
- Bioavailability:** Increased up to 82% when taken with a high-fat meal

Mechanism of Action

Nilotinib selectively inhibits the BCR-ABL tyrosine kinase formed due to the Philadelphia chromosome abnormality in chronic myeloid leukemia (CML). It binds to the ATP-binding site of the kinase, blocking downstream signaling pathways responsible for uncontrolled cell proliferation and survival. This inhibition induces apoptosis in malignant cells while sparing normal cells, offering improved specificity and reduced toxicity.

Dose

- Adults:** Newly diagnosed CML: 300 mg twice daily
- Resistant/intolerant CML: 400 mg twice daily

Pediatrics: 230 mg/m² twice daily (rounded to nearest 50 mg)

3.2. Bioflavonoid / Antioxidant Agent Profile

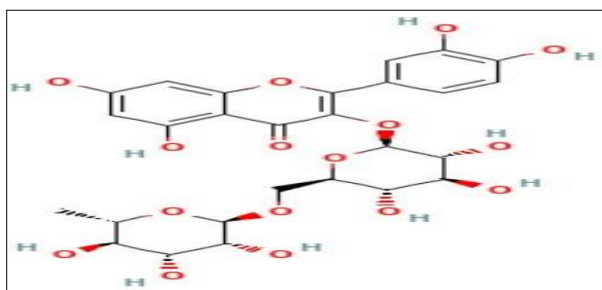
3.2.1 Rutin

Generic Name: Rutin

Synonyms: Phytomelin, Sophorin, Violaquercitrin, Globularicitrin

Molecular Formula: C₂₇H₃₀O₁₆

Molecular Weight: 610.52 g/mol



Melting Point: ~195°C (decomposes)

Description:

Rutin is a yellow crystalline, odorless bioflavonoid found in buckwheat, citrus fruits, tea, and apples, known for its antioxidant and vasoprotective properties.

Solubility: Poorly soluble in water; soluble in ethanol and pyridine.

Category: Bioflavonoid – Antioxidant and Anti-inflammatory agent.

Pharmacokinetics

- Absorption:** Poor intestinal absorption; metabolized by gut microflora
- Distribution:** Metabolites bind to plasma proteins (albumin)
- Metabolism:** Converted to quercetin and phenolic acids
- Excretion:** Primarily excreted in urine as metabolites

Mechanism of Action

Rutin exhibits potent antioxidant activity by scavenging free radicals and reducing oxidative stress. It strengthens capillaries by stabilizing collagen and elastin, decreases vascular permeability, and exhibits anti-inflammatory effects by inhibiting NF-κB activation and reducing COX-2 expression. These properties contribute to its anticancer, cardioprotective, and anti-inflammatory effects.

Dose: Common supplemental dose ranges from 200–600 mg/day, depending on therapeutic indication.

4. EXCIPIENTS PROFILE

4.1 Glyceryl Monostearate (GMS)

Generic Name: Glyceryl Monostearate

Synonyms: Glycerol Monostearate, Glyceryl Stearate

Molecular Formula: C₂₁H₄₂O₄

Molecular Weight: 358.56 g/mol

Melting Point: ~78°C

Description: Glyceryl Monostearate is a white, odorless, sweet-tasting flaky powder widely used in pharmaceutical formulations.

Solubility: Soluble in hot ethanol, ether, chloroform, hot acetone, mineral oil, and fixed oils; insoluble in water but dispersible with surfactants.

Category: Emulsifier, stabilizer, lubricant, and lipid matrix former.

Pharmacokinetics: GMS exhibits minimal systemic absorption. It is metabolized into glycerol and stearic acid and eliminated through normal metabolic pathways.

Mechanism of Action:

GMS possesses amphiphilic properties, enabling interaction with both aqueous and lipid phases. It reduces surface tension, stabilizes emulsions, and forms lipid monolayers at oil–water interfaces. In pharmaceutical formulations, GMS serves as a lipid matrix that enables controlled drug release by regulating diffusion through the solid lipid core. It also improves texture, consistency, and moisture retention.

Dose

- Controlled-release systems: 1–10% w/w
- Tablet lubricant: 0.5–2% w/w

4.2 Soy Lecithin (46)**Generic Name:** Soy Lecithin**Synonyms:** Lecithin (Soya), Soybean Lecithin**Molecular Formula:** $C_{42}H_{80}NO_8P$ **Molecular Weight:** 758.06 g/mol**Melting Point:** ~236.1°C**Description:**

Soy Lecithin is a yellow to brown semi-solid or powder obtained from soybeans. It contains phospholipids such as phosphatidylcholine and phosphatidylethanolamine.

Solubility: Soluble in chloroform, ether, and petroleum ether; insoluble in water and acetone.

Category: Excipient, emulsifier, stabilizer.

Pharmacokinetics

Soy lecithin shows limited systemic absorption. It is metabolized into fatty acids, glycerol, and choline derivatives and eliminated through normal metabolic pathways.

Mechanism of Action

Due to its amphiphilic phospholipid structure, soy lecithin reduces interfacial tension and stabilizes emulsions. It facilitates liposome formation, enhancing drug encapsulation, protection from degradation, and bioavailability. Lecithin integrates with biological membranes, improving cellular uptake and controlled drug release in nanoparticulate systems.

Dose

- Excipient in formulations: 1–5% w/w
- Liposomal systems: formulation-dependent

4.3 Dimethyl Sulfoxide (DMSO)**Generic Name:** Dimethyl Sulfoxide**Synonyms:** DMSO, Methanesulfinylmethane**Molecular Formula:** C_2H_6OS **Molecular Weight:** 78.13 g/mol**Melting Point:** ~19°C

Description: DMSO is a colorless, highly polar aprotic solvent with a characteristic odor, known for its exceptional membrane penetration ability.

Solubility: Miscible with water, ethanol, acetone, chloroform, and most organic solvents.

Category: Solvent, cryoprotectant, anti-inflammatory agent.

Pharmacokinetics: Rapidly absorbed through skin and mucosa; metabolized to dimethyl sulfone and excreted

via urine and breath.

Mechanism of Action:

DMSO enhances membrane permeability, facilitating drug transport. It acts as a cryoprotectant by preventing ice crystal formation and exhibits anti-inflammatory, antioxidant, analgesic, and antimicrobial properties. Its solvent capacity allows dissolution of poorly soluble drugs, improving formulation efficiency.

Dose

- Topical use: 50–90%
- Cryopreservation: ~10%

4.4 Ethanol**Generic Name:** Ethanol**Synonyms:** Ethyl Alcohol, Grain Alcohol**Molecular Formula:** C_2H_6O **Molecular Weight:** 46.07 g/mol**Melting Point:** ~114.1°C

Description: Ethanol is a clear, volatile liquid widely used as a solvent and antiseptic in pharmaceutical preparations.

Solubility: Miscible with water, ether, chloroform, and acetone.

Category: Pharmaceutical solvent and antiseptic.

Pharmacokinetics

Rapid absorption; metabolized in the liver to acetaldehyde and acetic acid; excreted via breath, urine, and sweat.

Mechanism of Action:

Ethanol alters membrane fluidity and acts as a solvent for drug dissolution. At the CNS level, it modulates GABA and NMDA receptors, producing sedative effects. In formulations, ethanol enhances solubility and penetration of active ingredients.

Dose: Clinical dosing varies depending on therapeutic indication.

4.5 Methanol**Generic Name:** Methanol**Synonyms:** Methyl Alcohol, Wood Alcohol**Molecular Formula:** CH_3OH **Molecular Weight:** 32.04 g/mol**Melting Point:** ~97.6°C

Description: Methanol is a volatile, flammable liquid used primarily as an industrial solvent and chemical intermediate.

Solubility: Miscible with water, ethanol, acetone, and organic solvents.

Category: Industrial solvent and chemical precursor.

Pharmacokinetics & Toxicity:

Methanol is rapidly absorbed and metabolized to formaldehyde and formic acid, which cause metabolic acidosis, optic nerve damage, and CNS depression. Ethanol or fomepizole acts as an antidote by inhibiting

alcohol dehydrogenase.

Dose: Toxic dose >10 mL; not intended for pharmaceutical use.

5. PLAN OF WORK

Pre-Formulation Study

- Determination of melting point
- Solubility study
- Calibration curve
- Compatibility using FTIR

Dose fixing of Nilotinib and rutin for SLNs

- *In vitro* cytotoxicity study of nilotinib
- *In vitro* cytotoxicity study of nilotinib and Nilotinib and rutin loaded SLNs

- Entrapment efficacy

Preparation of SLNs

Evaluation of SLNs

- Drug content
- *In vitro* dissolution studies
- Particle size, poly dispersity index and zetapotential
- Surface morphology

In vitro cell line studies

- Cell cycle analysis
- Cell apoptosis analysis

6. MATERIALS AND METHODS

6.1 Materials and Suppliers

Table 1: Materials and Suppliers

S. No	Material	Supplier
1	Nilotinib	Sigma-Aldrich
2	Rutin	Sigma-Aldrich
3	Glyceryl Monostearate	Sigma-Aldrich
4	Soy Lecithin	Loba Chemie
5	DMSO	Aldrich Co.
6	Ethanol	Aldrich Co.
7	Methanol	Aldrich Co.

6.2 Instruments and Apparatus

Table 2: Instruments and Equipment

S. No	Instrument	Manufacturer / Model
1	Digital balance	Shimadzu (BL-220H)
2	Dissolution apparatus	Labindia (Disso 2000)
3	FTIR Spectrophotometer	Shimadzu (FTIR-8400S)
4	Glassware	Sigma Scientific Glass Pvt. Ltd
5	Melting point apparatus	SESW
6	Magnetic stirrer	REMI (2 MLH)
7	Mechanical stirrer	REMI (RQ-121/D)
8	Particle size analyzer	AccuSizer 780
9	SEM	Hitachi (S-450)
10	Stability chamber	REMI (CHM-10S)
11	UV-Visible Spectrophotometer	Shimadzu
12	Flow Cytometer	DxFLEX, Beckman Coulter

6.3 Pre-Formulation Studies

Pre-formulation studies were conducted to evaluate the physicochemical properties of Nilotinib and Rutin, including melting point, solubility, and compatibility, to ensure formulation stability and performance.

6.3.1 Melting Point

Melting points were determined using the capillary tube method. Drug samples were packed in capillary tubes and analyzed using a melting point apparatus.

6.3.2 Solubility Study

Solubility was assessed by dissolving 1 mg of drug in 10 mL of various solvents followed by orbital shaking for 24 hours. Drug concentration was determined using UV-Visible spectrophotometry.

6.4 Calibration Curve

6.4.1 Nilotinib

Standard solutions (10–70 µg/mL) were prepared from a 100 µg/mL stock in DMSO. Absorbance was measured at 263 nm.

6.4.2 Rutin

Rutin stock solution (100 µg/mL) was prepared in ethanol and diluted to obtain concentrations of 10–100 µg/mL. Absorbance was measured at 207 nm.

6.4.3 FTIR Compatibility Study

FTIR analysis was performed using the KBr pellet method over 400–4000 cm⁻¹ to detect drug-excipient interactions.

6.5 Dose Fixing and Cytotoxicity Studies

6.5.1 In-vitro Cytotoxicity of Nilotinib

MDA-MB-231 cells were cultured in DMEM-HG and treated with Nilotinib (10–100 µg/mL). Cell viability was assessed using the MTT assay and IC₅₀ was determined.

6.5.2 Cytotoxicity of Nilotinib–Rutin and SLNs

Cells were treated with IC₅₀ concentration of Nilotinib (33 µg/mL) combined with varying Rutin concentrations. Cell viability was evaluated using the MTT assay.

6.6 Preparation of Nilotinib-Loaded SLNs

SLNs were prepared using hot emulsification followed by probe sonication. Nilotinib and Rutin were dissolved with Glyceryl Monostearate in chloroform: methanol (1:1). After solvent evaporation and lipid melting, an aqueous surfactant phase was added, sonicated, and cooled to form SLNs.

Table 3: Method for Synthesizing Nilotinib-Loaded SLN:

Formulation	Nilotinib (mg)	Rutin (mg)	glyceryl mono stearate (%)	Soy Lecithin (%)	Cremophor RH40 (%)	methanol &chloroform (1:) ml	Water (ml)
F1	200	151.5	4	4	3	20	qs
F2	200	151.5	8	4	3	20	qs
F3	200	151.5	4	4	9	20	qs
F4	200	151.5	6	4	6	20	qs
F5	200	151.5	4	2	4	20	qs
F6	200	151.5	8	2	3	20	qs
F7	200	151.5	4	6	5	20	qs
F8	200	151.5	8	6	6	20	qs
F9	200	151.5	6	2	3	20	qs
F10	200	151.5	6	2	9	20	qs
F11	200	151.5	6	6	3	20	qs
F12	200	151.5	6	6	9	20	qs

6.7 Evaluation of SLNs

6.7.1 Entrapment Efficiency

SLNs were centrifuged at 20,000 rpm and free drug in the supernatant was quantified by UV spectrophotometry at 263 nm.

6.7.2 Drug Content

SLNs equivalent to 5 mg drug were dissolved in 0.1 N HCl: ethanol (3:1) and analyzed spectrophotometrically.

6.7.3 In-Vitro Drug Release

Dialysis bag diffusion method was used in 0.1 N HCl: ethanol (3:1) at 37°C. Samples were analyzed at 263 nm (Nilotinib) and 207 nm (Rutin).

6.7.4 Particle Size, PDI & Zeta Potential

Measured using dynamic light scattering (Anton Paar Litesizer DLS 500).

6.7.5 Surface Morphology

SEM analysis was conducted after gold-palladium sputter coating.

6.8 Cell Cycle and Apoptosis Analysis

6.8.1 Cell Cycle Analysis

PI staining followed by flow cytometry was used to analyze cell cycle arrest in treated MDA-MB-231 cells.

6.8.2 Apoptosis Study

Annexin V-PE assay was performed to quantify apoptosis using flow cytometry.

7. RESULTS AND DISCUSSION

7.1 Pre-Formulation Studies

7.1.1 Melting Point

The melting points of nilotinib and rutin were determined using the capillary tube method to assess purity and thermal stability. Nilotinib exhibited a melting point of 232°C, consistent with reported literature values, confirming its purity and stability. Rutin showed a melting point of 125°C, aligning with standard references. These results indicate that both compounds possess acceptable physicochemical stability for formulation development.

7.1.2 Solubility Studies

Nilotinib was found to be insoluble in water and

sparingly soluble in methanol and ethanol, reflecting its hydrophobic nature. However, it showed good solubility in DMSO and 0.1 N HCl: ethanol (3:1), likely due to protonation of basic functional groups. Rutin exhibited sparing solubility in water but was freely soluble in

methanol and ethanol, attributed to its polyhydroxylated flavonoid structure. Both drugs were soluble in DMSO and acidic ethanolic media, supporting their suitability for SLN formulation.

Table 4: Solubility of nilotinib and rutin

Solvent	Solubility of nilotinib	Solubility of rutin
Distilled water	Insoluble	Sparingly soluble
Methanol	Sparingly soluble	Freely soluble
Ethanol	Sparingly soluble	Freely soluble
DMSO	Soluble	Soluble
0.1N HCl (pH 1.2): ethanol (3:1)	Soluble	Soluble

7.1.3 Calibration Curves

UV spectrophotometric calibration curves for nilotinib (263 nm) and rutin (207 nm) demonstrated excellent linearity over their respective concentration

ranges.

- **Nilotinib:** $y = 0.0084x - 0.008$, $R^2 = 0.999$

Table 5: Calibration curve of nilotinib

Concentration ($\mu\text{g/mL}$)	Absorbance
0	0
10	0.096
20	0.175
40	0.346
60	0.519
80	0.667

Calibration curve of Nilotinib

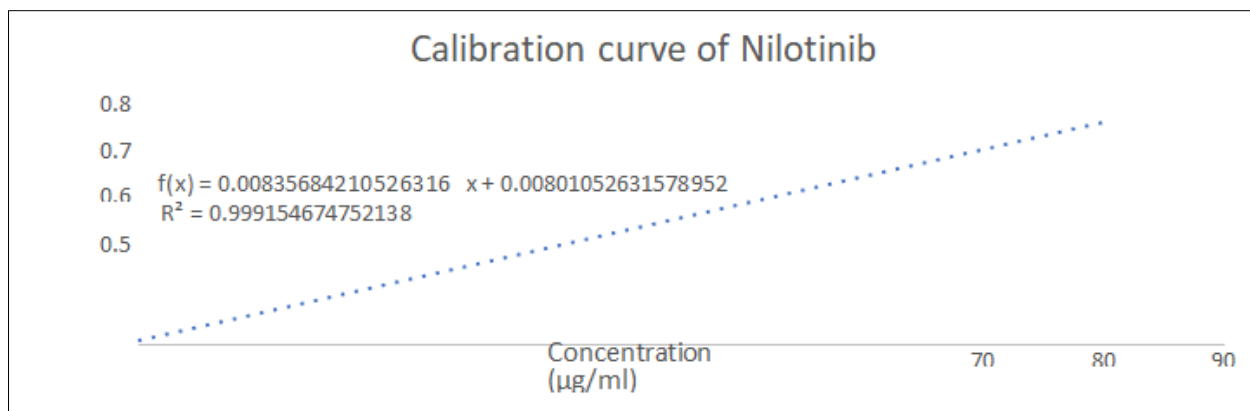


Figure No: 1 Standard curve of Nilotinib

- **Rutin:** $y = 0.0128x - 0.0013$, $R^2 = 0.999$

These results confirm the reliability of the analytical method for quantitative estimation.

Table 6: Calibration curve of rutin

Rutin concentration ($\mu\text{g/ml}$)	Absorbance
0	0
10	0.117
20	0.243
30	0.371
40	0.492
50	0.623
60	0.771
70	0.892

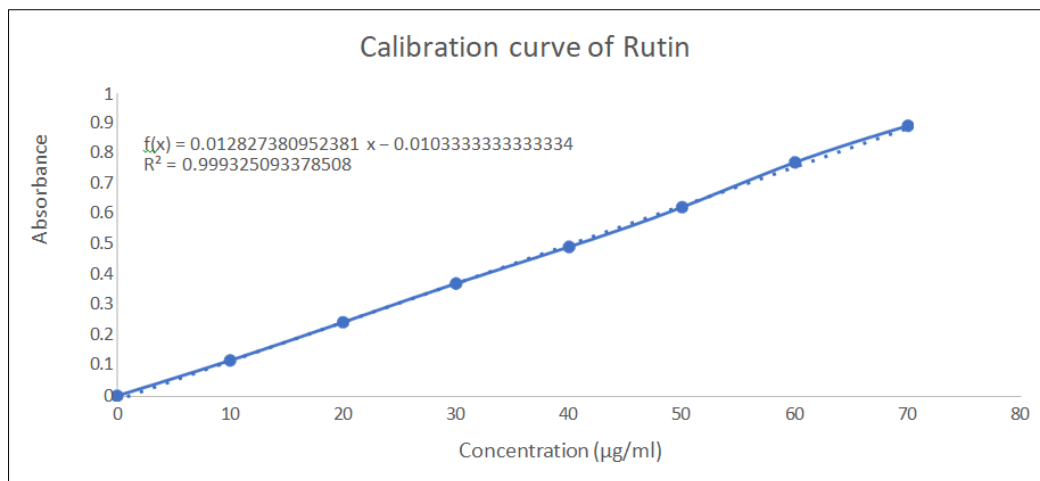


Figure No: 2 Standard curve of Rutin

7.1.4 Compatibility Study (FTIR)

FTIR spectra of nilotinib, rutin, excipients (GMO, Cremophor RH40, soy lecithin), and their physical mixture showed characteristic peaks

corresponding to their functional groups. The absence of peak shifts or new peaks in the physical mixture indicates no chemical interaction, confirming compatibility among formulation components.

Table 7: Compatibility study using FTIR

Functional groups	Nilotinib	Rutin	GMO	Cremophor RH 40	Soy lecithin	Physical mixture
O-H stretching	3139.25	3423.41	3036.06	2942.51	2946.36	3132.50
C-H stretching	2828.70	2937.38	2848.96	2359.98	2355.16	2775.66
C=O stretching	1659.80		1675.49	1652.95	1655.94	1679.09
-CH ₃ bending			1464.02	1461.13		1414.83
C-H bending	751.30	1654.81	736.83	776.37	799.52	801.45
Aromatic C-H bending		1456.16				1505.49
C=C bending	883.43	808.12				879.57
Amide stretching	1700.31					1700.31
C-F stretching	1259.80					1257.63

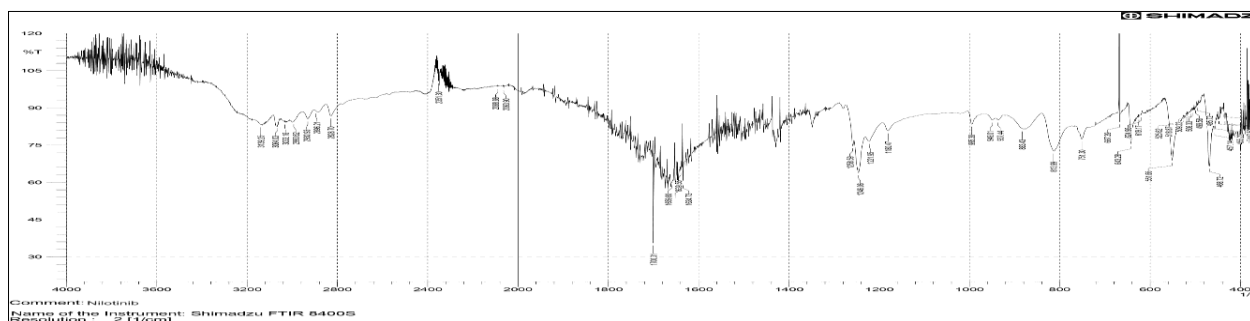


Figure No 3: FTIR spectra of Nilotinib

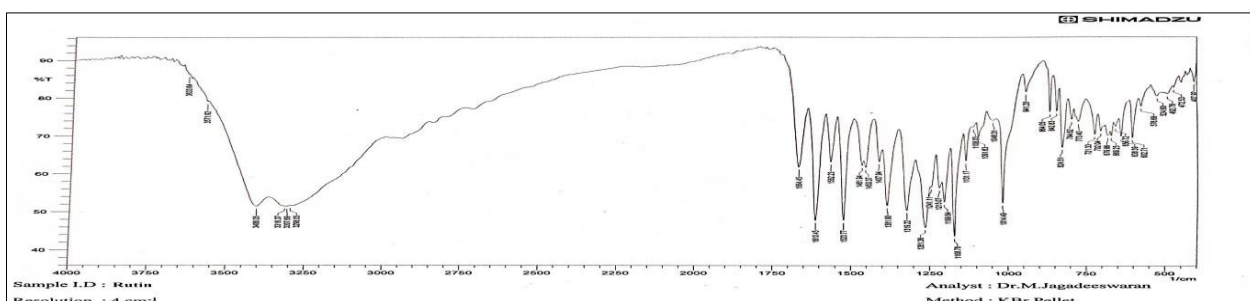


Figure No 4: FTIR spectra of Rutin

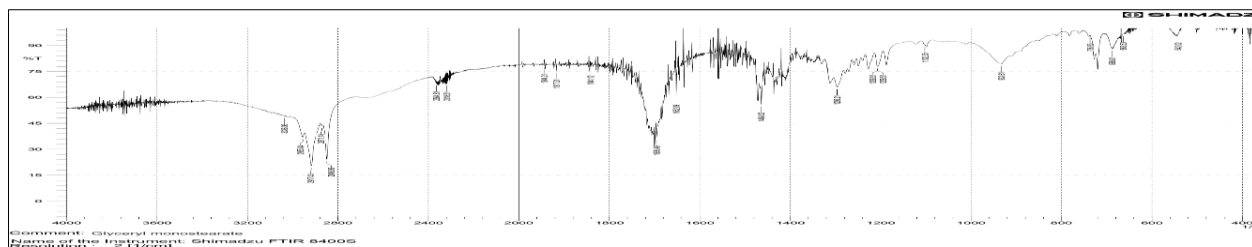


Figure No 5: FTIR spectra of glyceryl monostearate

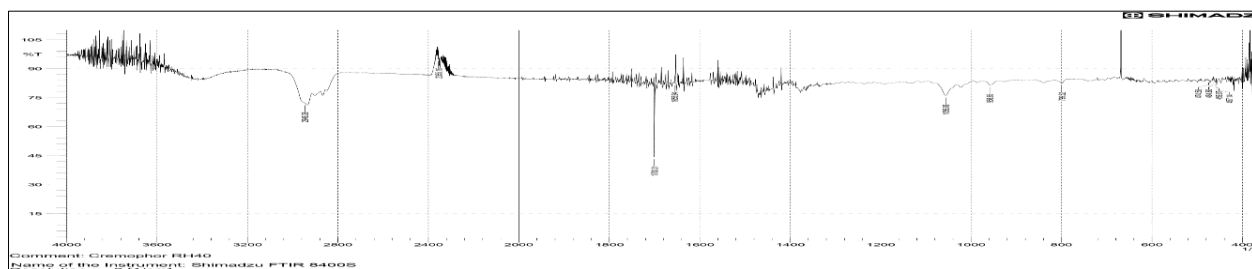


Figure No 6: FTIR spectra of Cremophor RH40

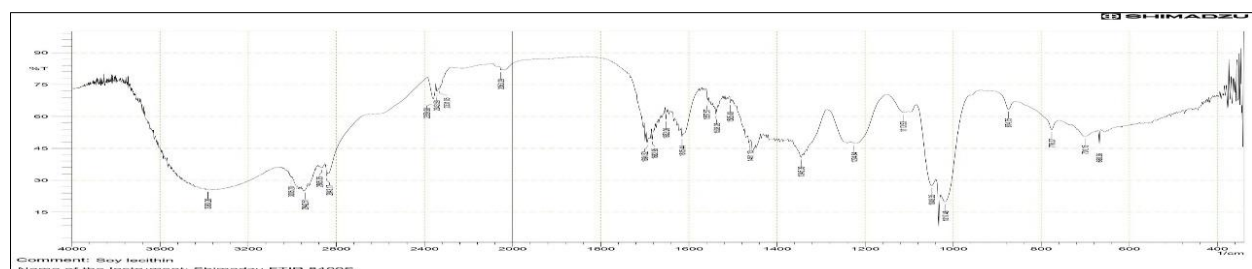


Figure No 7: FTIR spectra of soy lecithin

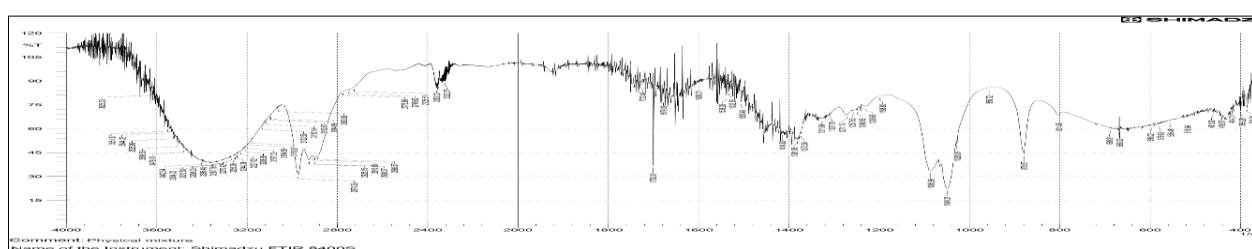


Figure No 8: FTIR spectra of physical mixture

7.2 Dose Fixing and Cytotoxicity Studies

7.2.1 In vitro Cytotoxicity of Nilotinib

Nilotinib exhibited a dose-dependent cytotoxic effect against MDA-MB-231 breast cancer cells. The

IC₅₀ value was determined to be 33 µg/mL, confirming its antiproliferative activity.

Table 8: *In vitro* cytotoxicity study of nilotinib

Concentration (µg/ml)	% Viability
Control	100
10µg/ml	67.5953708
20µg/ml	63.6590942
30µg/ml	53.857694
40µg/ml	40.9844263
50µg/ml	39.7342477
60µg/ml	37.2624661
70µg/ml	32.1045864
80µg/ml	26.4394914
90µg/ml	11.9302758

Concentration ($\mu\text{g/ml}$)	% Viability
100 $\mu\text{g/ml}$	8.17259609

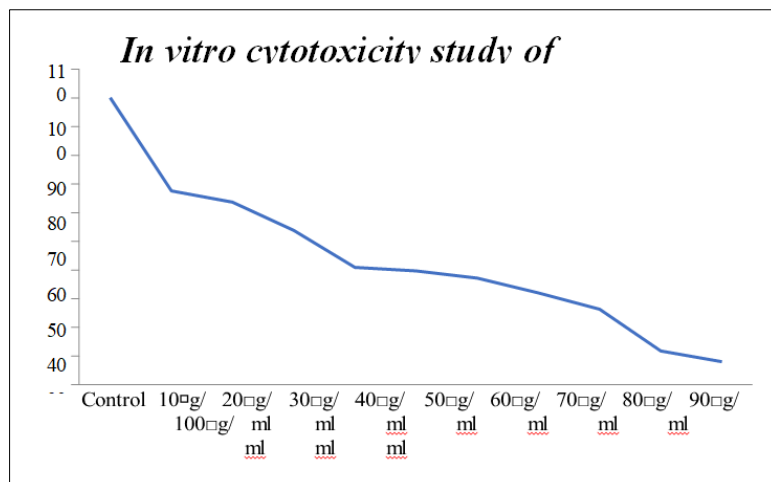
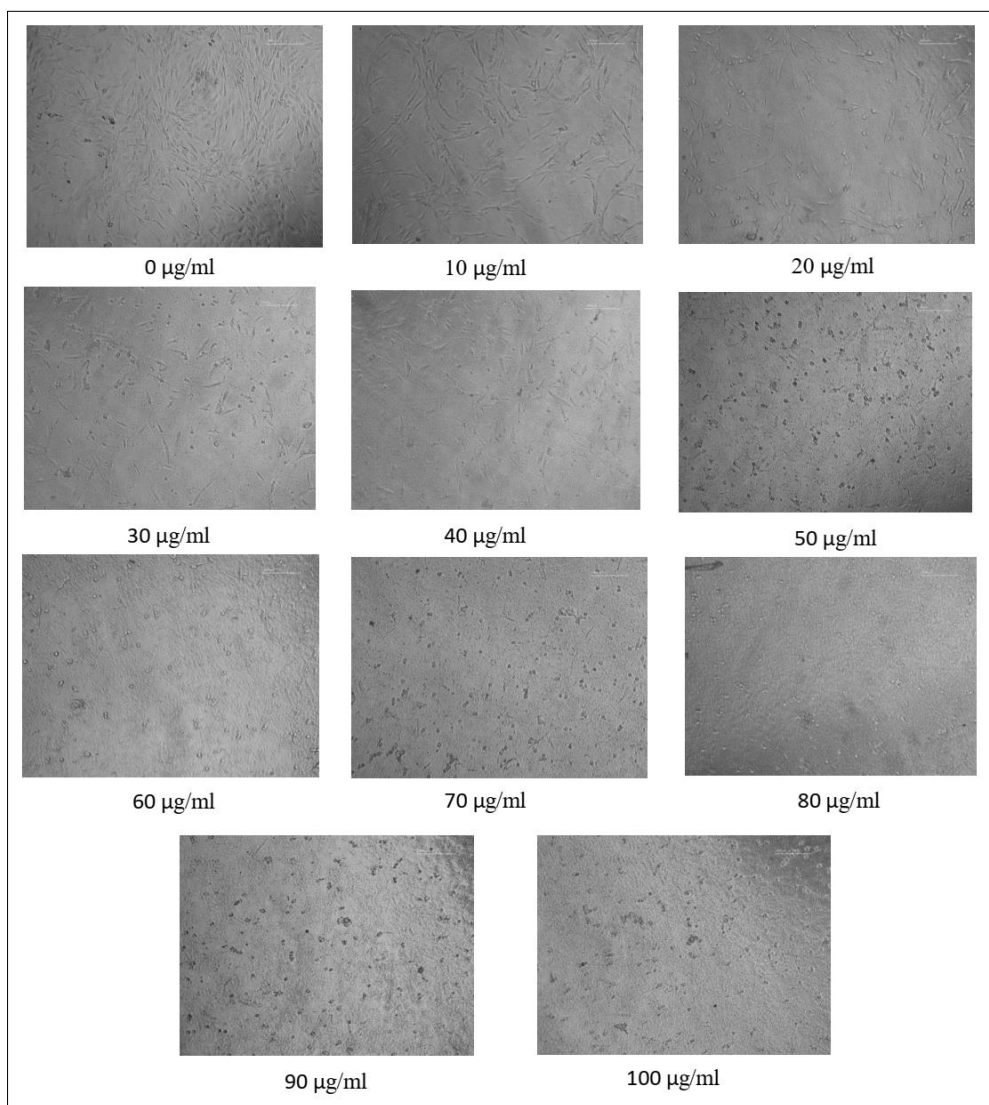


Figure No 9: *In-vitro* cytotoxicity study of Nilotinib



7.2.2 Cytotoxicity of Nilotinib–Rutin Combination

The combination of nilotinib (33 $\mu\text{g/mL}$) with

increasing concentrations of rutin enhanced cytotoxicity compared to nilotinib alone. The IC_{50} of the combination

decreased to 23 $\mu\text{g}/\text{mL}$, indicating a synergistic or additive effect. Higher rutin concentrations significantly

reduced cell viability, demonstrating its sensitizing role.

Table 9: Cytotoxic effect of the nilotinib and rutin combination

Nilotinib IC50	Rutin	% Viability
33 $\mu\text{g}/\text{ml}$	0 $\mu\text{g}/\text{ml}$	100
33 $\mu\text{g}/\text{ml}$	1 $\mu\text{g}/\text{ml}$	98.421
33 $\mu\text{g}/\text{ml}$	2 $\mu\text{g}/\text{ml}$	98.324
33 $\mu\text{g}/\text{ml}$	3 $\mu\text{g}/\text{ml}$	96.765
33 $\mu\text{g}/\text{ml}$	4 $\mu\text{g}/\text{ml}$	96.254
33 $\mu\text{g}/\text{ml}$	5 $\mu\text{g}/\text{ml}$	91.583
33 $\mu\text{g}/\text{ml}$	10 $\mu\text{g}/\text{ml}$	75.433
33 $\mu\text{g}/\text{ml}$	15 $\mu\text{g}/\text{ml}$	68.427
33 $\mu\text{g}/\text{ml}$	20 $\mu\text{g}/\text{ml}$	57.059
33 $\mu\text{g}/\text{ml}$	25 $\mu\text{g}/\text{ml}$	43.310
33 $\mu\text{g}/\text{ml}$	50 $\mu\text{g}/\text{ml}$	9.938

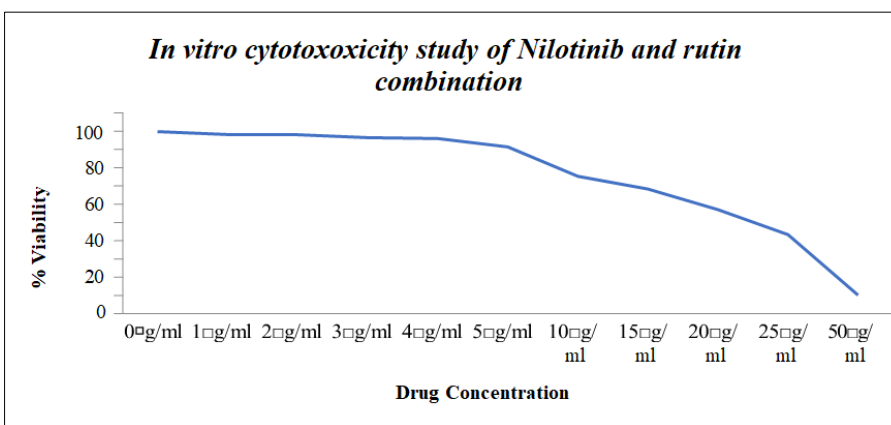
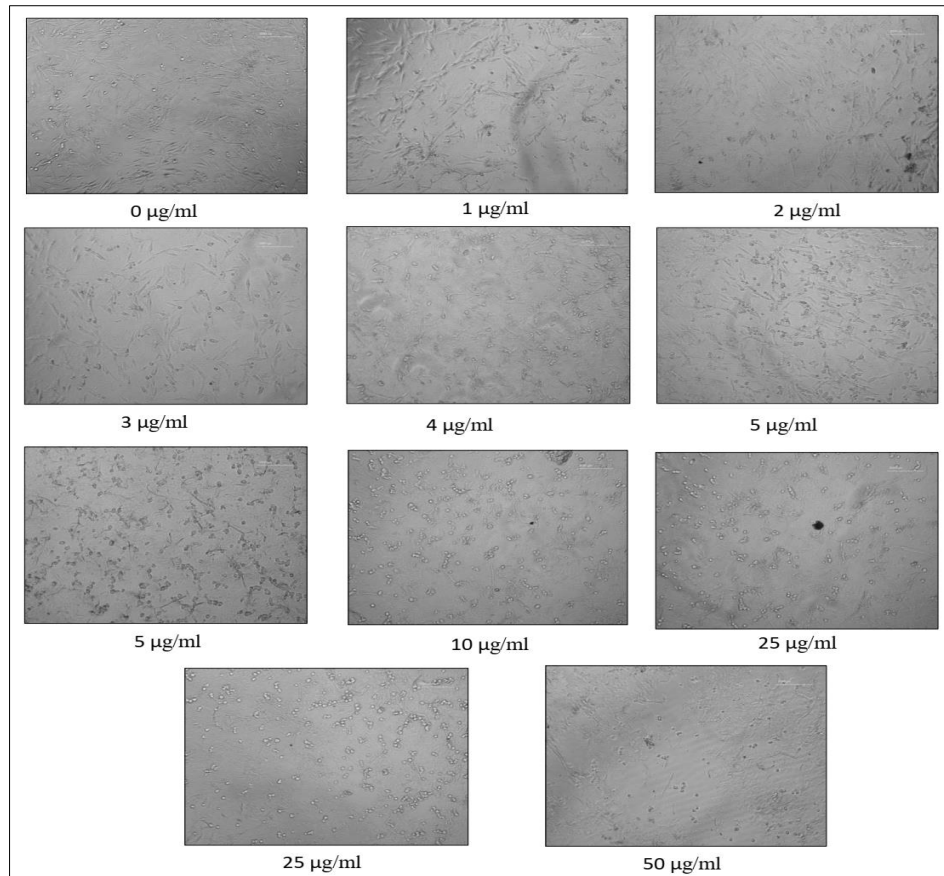


Figure No 10: *In-vitro* cytotoxicity study of Nilotinib and rutin combination



7.3 Preparation and Optimization of SLNs

Twelve formulations (F1–F12) were prepared by varying lipid and surfactant concentrations. Formulations F1–F2 showed immediate phase separation, while F3–F6 were stable with slight turbidity.

Formulations F7–F12 separated upon storage. Formulation F5 showed optimal physical stability, highest entrapment efficiency, and drug content, and was selected for further evaluation.

Table 10: Nilotinib and rutin-loaded SLNs with visual observation

Formulation	Visual observation
F1	Separation
F2	Separation
F3	Slightly turbid liquid
F4	Slightly turbid liquid
F5	Slightly turbid liquid
F6	Slightly turbid liquid
F7	Slightly turbid liquid, separated on storage
F8	Slightly turbid liquid, separated on storage
F9	Slightly turbid liquid, separated on storage
F10	Slightly turbid liquid, separated on storage
F11	Slightly turbid liquid, separated on storage
F12	Slightly turbid liquid, separated on storage

7.4 Evaluation of SLNs

7.4.1 Entrapment Efficiency and Drug Content

Entrapment efficiency varied widely across

formulations. F5 showed the highest entrapment efficiency (89%) and drug content (99.98%), indicating efficient drug incorporation and minimal loss.

Table 11: % entrapment efficacy of SLN

Trial	% entrapment efficacy
F1	22
F2	31
F3	67

F4	76
F5	89
F6	70
F7	Separated
F8	Separated
F9	Separated
F10	Separated
F11	Separated
F12	Separated

7.4.2 In vitro Drug Release

Both nilotinib and rutin exhibited a biphasic release pattern, characterized by an initial burst followed by

sustained release up to 24 hours.

- **Nilotinib:** ~99.8% release at 24 hr

Table 12: In vitro drug release from SLNs

Time (h)	Absorbance	Conc (μ /ml)	Conc (mg/ml)	Conc*df	Error	Bath Conc	Drug rls	% DR
0	0	0	0	0	0	0	0	0
1	0.265	32.08	0.03	0.32	0.32	11.23	11.55	23.09
3	0.415	50.83	0.05	0.51	0.83	17.79	18.62	37.24
6	0.552	67.95	0.07	0.68	1.51	23.78	25.29	50.58
9	0.679	83.83	0.08	0.84	2.35	29.34	31.69	63.37
12	0.788	97.45	0.10	0.97	3.32	34.11	37.43	74.86
16	0.887	109.83	0.11	1.10	4.42	38.44	42.86	85.72
20	0.954	118.20	0.12	1.18	5.60	41.37	46.97	93.94
24	0.993	123.08	0.12	1.23	6.83	43.08	49.91	99.82

- **Rutin:** ~99.9% release at 24 h

This sustained release profile suggests effective

entrapment within the lipid matrix and controlled diffusion.

Table 13: Rutin release from SLNs

Time (h)	Absorbance	Con. (μ g/ml)	Con. (mg/ml)	Con*df	Error	Bath Con.	Drug Rls.	% DR
0	0	0	0	0	0	0	0	0
1	0.201	14.90	0.01	0.15	0.15	5.21	5.36	21.45
3	0.322	24.35	0.02	0.24	0.39	8.52	8.92	35.66
6	0.439	33.49	0.03	0.33	0.73	11.72	12.45	49.80
9	0.551	42.24	0.04	0.42	1.15	14.78	15.93	63.74
12	0.658	50.60	0.05	0.51	1.66	17.71	19.37	77.47
16	0.734	56.54	0.06	0.57	2.22	19.79	22.01	88.04
20	0.769	59.27	0.06	0.59	2.81	20.75	23.56	94.24
24	0.799	61.62	0.06	0.62	3.43	21.57	25.00	99.98

7.4.3 Drug Release Kinetics

Release data best fitted the Higuchi model for both drugs (Nilotinib $R^2 = 0.989$; Rutin $R^2 = 0.992$), indicating diffusion-controlled release from the SLN matrix.

revealed spherical particles with smooth surfaces, confirming successful SLN formation.

7.6 Cell Cycle and Apoptosis Analysis

7.6.1 Cell Cycle Arrest

Nilotinib, its combination with rutin, and SLN formulations induced significant G1 phase arrest in MDA-MB-231 cells compared to control. This indicates inhibition of cell cycle progression as a key mechanism of anticancer activity.

7.5 Particle Size, Zeta Potential, and Morphology

The optimized SLN formulation exhibited a mean particle size of 360.5 nm, PDI of 0.238, and zeta potential of -31.7 mV, indicating a uniform size distribution and good colloidal stability. SEM analysis

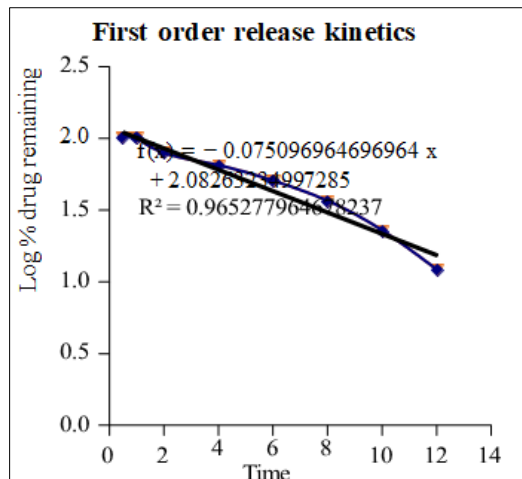


Figure No 11: First order release (Nilotinib)

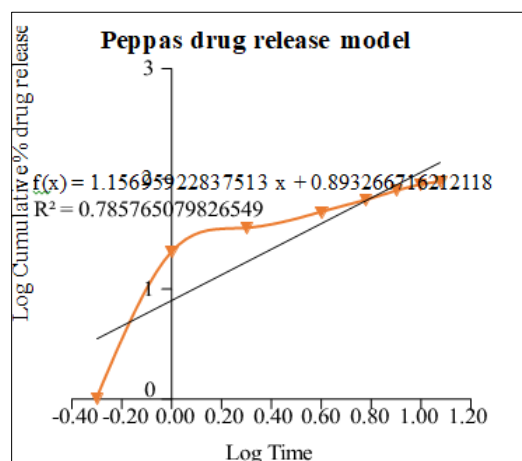


Figure No 12: Peppas's release (Nilotinib)

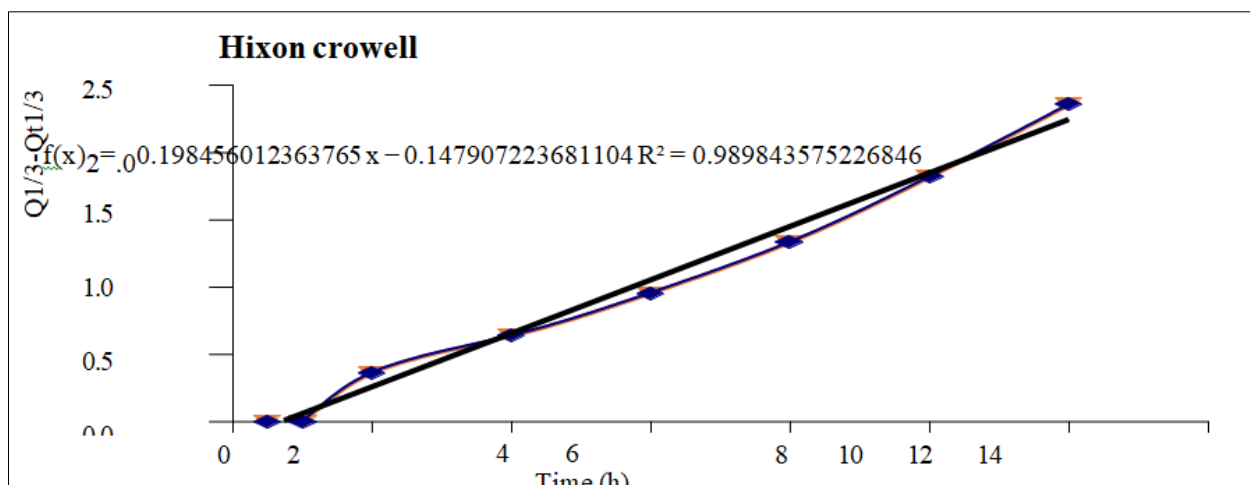


Figure No 13: Hixon crowell release (Nilotinib)

Table 14: Drug release kinetics of Nilotinib:

Release kinetics	Zero order model	First order model	Higuchi model	Kors Mayer Peppas model	Hixon Crowell model
R ² value	0.853	0.975	0.989	0.9781	0.975

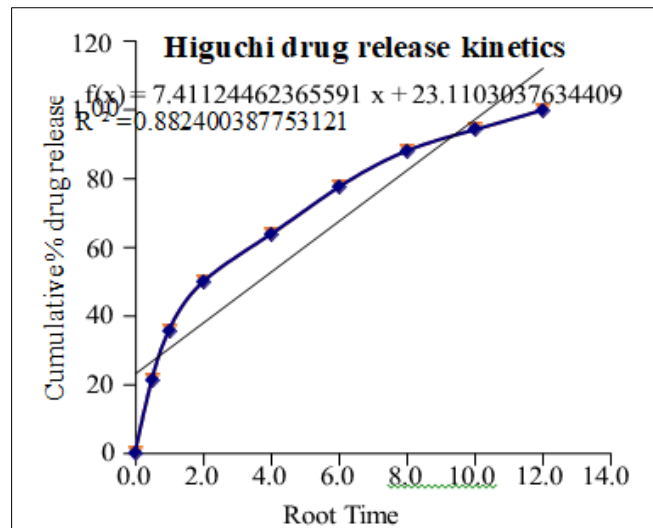


Figure No 14: Higuchi release (Rutin)

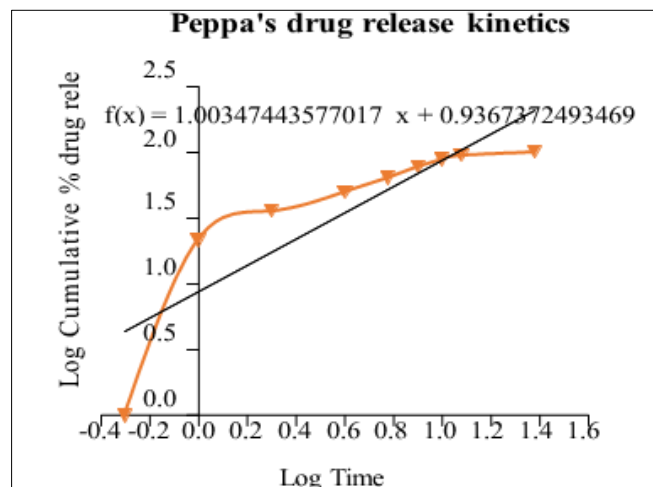


Figure No 15: Peppa's release (Rutin)

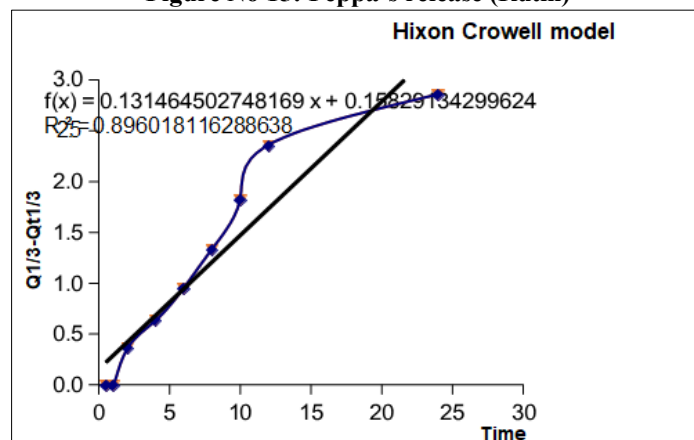


Figure No 16: Hixon crowell release (Rutin)

Table 15: Drug release kinetics of Rutin

Release kinetics	Zero order model	First order model	Higuchi model	Kors Mayer Peppas model	Hixon Crowell model
R2 value	0.7108	0.9419	0.9924	0.7498	0.896

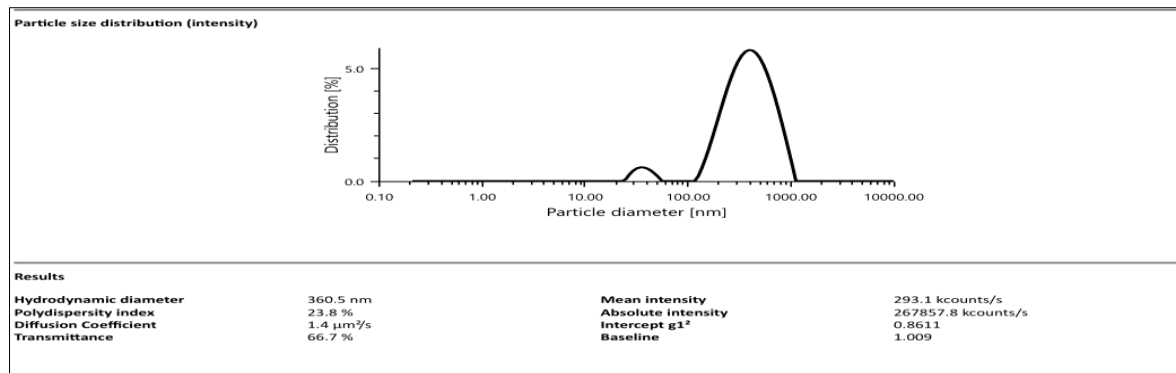


Figure No 17: Particle size distribution (Intensity)

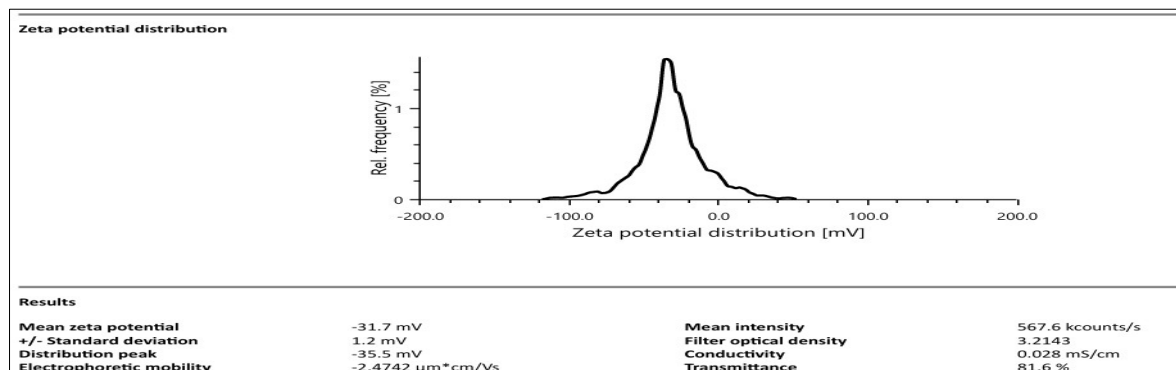


Figure No 18: Zeta potential distribution

7.6.2 Apoptosis Analysis

Flow cytometry showed that nilotinib induced apoptosis, which was further enhanced by rutin and maximized in the nilotinib–rutin SLN formulation. The SLN group showed the lowest viable cell population and highest early and late apoptosis, demonstrating improved

therapeutic efficacy through nanoparticle delivery.

For Nilotinib and its Rutin-enhanced formulation in targeting MDA-MB-231 breast cancer cells.

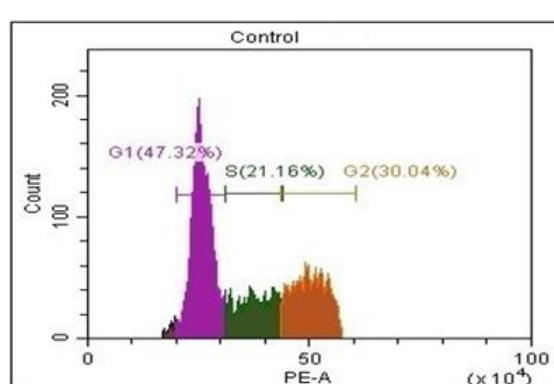
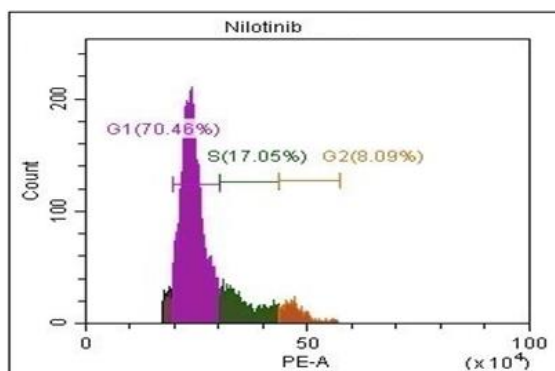
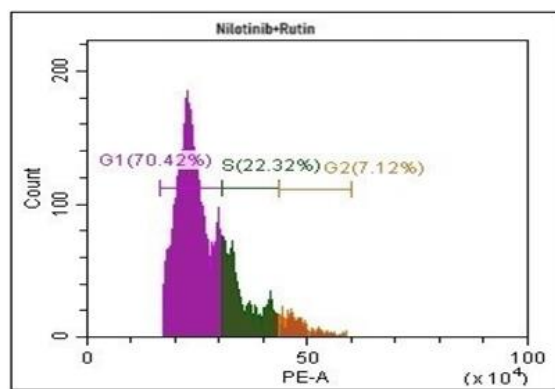
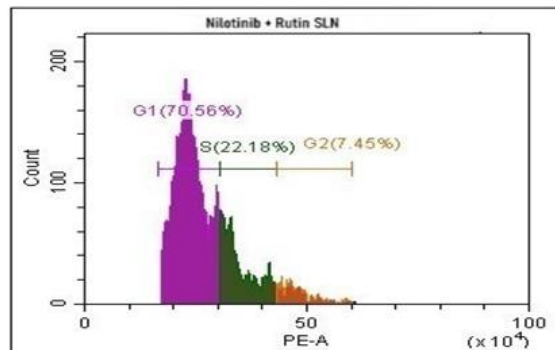
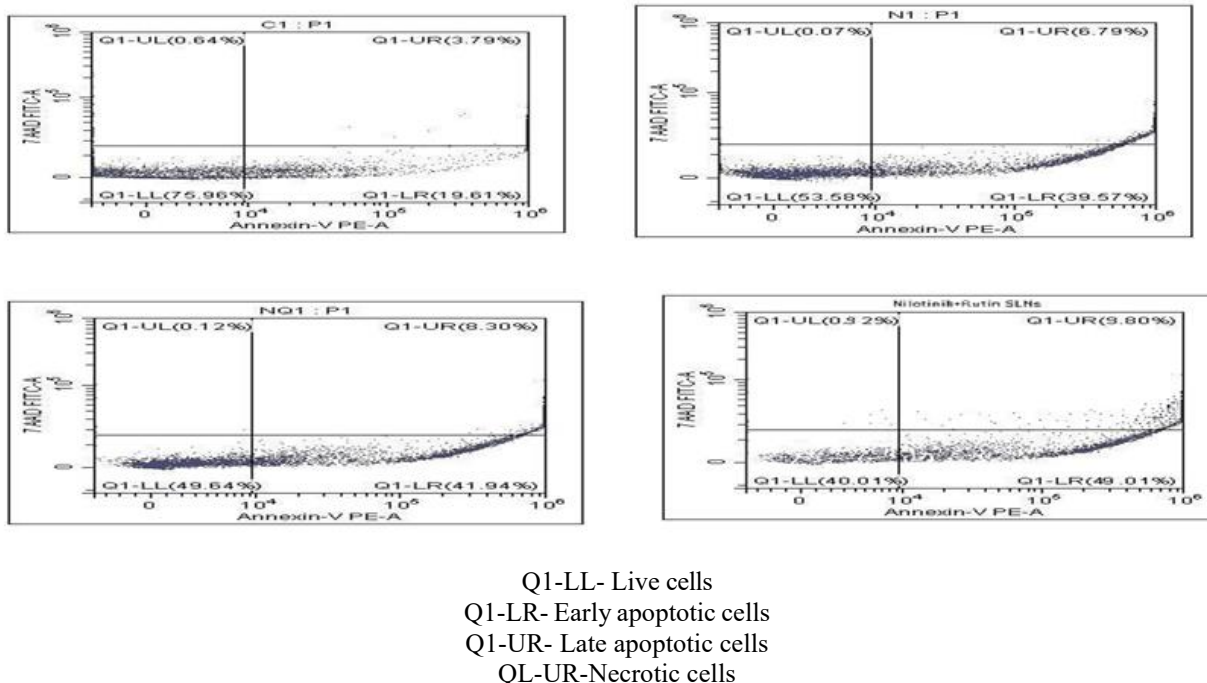


Figure No 25: G1 Phase inhibition**Figure No 26: G1 Phase inhibition (Control) (Nilotinib)****Figure No 27: G1 Phase inhibition****Figure No 28: G1 Phase inhibition (Nilotinib+Rutin) (Nilotinib+Rutin SLN)****Table 16: Cell cycle analysis**

Category	G1 Phase (%)	S Phase (%)	G2 Phase (%)
Control	54.19%	95.88%	30.04%
Nilotinib	70.46%	17.05%	8.09%
Nilotinib+Rutin (33:25)	70.42%	22.32%	7.12%
Nilotinib+Rutin SLN	70.56%	22.18%	7.45%



8. CONCLUSION

The co-delivery of Nilotinib and Rutin through SLN signifies a transformative approach to cancer therapy, combining advanced drug delivery technology with the therapeutic potential of these two agents. This novel strategy is designed to optimize treatment outcomes by addressing key challenges such as drug solubility, bioavailability, and systemic toxicity.

Enhanced Therapeutic Efficacy:

Encapsulating Nilotinib and Rutin in SLN improves their absorption and ensures controlled release. This targeted delivery increases drug bioavailability, concentrates the therapy at tumor sites, and minimizes harm to healthy tissues. Together, Nilotinib and Rutin enhance anti-cancer effects through their complementary actions, making the combination highly effective.

Mitigation of Toxicity:

A significant limitation of conventional cancer treatments is the severe toxicity associated with systemic drug administration. SLNs serve as a biocompatible and biodegradable vehicle, safeguarding the drugs during transit and ensuring their release specifically at the target site.

Advantages of SLNs:

Improved Stability: SLNs protect the encapsulated drugs from degradation caused by environmental factors like light, pH, and enzymatic activity.

Controlled Drug Release: The nanoparticles facilitate a sustained release profile, allowing consistent therapeutic levels of the drugs over an extended period.

Targeted Delivery: Surface modifications can further enhance tumor-targeting capabilities, such as through the addition of ligands or antibodies that bind specifically to cancer cell receptors.

Addressing Limitations of Conventional Systems: Traditional drug delivery systems face challenges like poor drug solubility, quick removal from the body, and lack of targeted action. SLNs solve these issues by providing a flexible, adaptable solution that suits the drugs' properties and biological conditions.

In Conclusion this strategy presents a comprehensive solution to the persistent challenges of cancer therapy, merging innovative drug delivery with the therapeutic benefits of Nilotinib and Rutin.

REFERENCES

1. National Cancer Institute: A comprehensive resource for understanding cancer. Link: <https://www.cancer.gov/about-cancer/understanding/what-is-cancer>.
2. National Center for Biotechnology Information (NCBI): A detailed article on the cell cycle and cancer is available on their site. Link: <https://www.ncbi.nlm.nih.gov/>
3. Nature Reviews Cancer: Offers insights into cancer biology, including the interplay between genetic mutations, tumor suppressor genes, and oncogenes. Website: <https://www.nature.com/nrc/>.
4. American Cancer Society (ACS): Provides information on apoptosis, cancer development, and related cellular mechanisms. Link: <https://www.cancer.org/>
5. Dai X, Shen L, Zhang J. Cold atmospheric plasma:

- redox homeostasis to treat cancers? *Trends Biotechnol.* 2023;41(1):15–8. <https://doi.org/10.1016/j.tibtech.2022.07.007>.
6. Danielsson, Frida, McKenzie Kirsten Peterson, Helena Caldeira Araújo and Franziska Lautenschläger, et al. "Vimentin diversity in health and disease." *Cells* 7 (2018): 147.
 7. Baldovini, Chiara, Giulio Rossi and Alessia Ciarrocchi. "Approaches to tumor classification in pulmonary sarcomatoid carcinoma." *Lung Cancer* (2019): 131-149.
 8. Kidd, Martha E., Dale K. Shumaker and Karen M. Ridge. "The role of vimentin intermediate filaments in the progression of lung cancer." *Am J Respir Cell Mol Biol* 50 (2014): 1-6.
 9. Zhang, Yujie and Branko Stefanovic. "LARP6 meets collagen mRNA: specific
 10. Global Burden of Disease 2019 Cancer Collaboration; Kocarnik JM, Compton K, et al. Cancer Incidence, Mortality, Years of Life Lost, Years Lived With Disability, and Disability-Adjusted Life Years for 29 Cancer Groups From 2010 to 2019: A Systematic Analysis for the Global Burden of Disease Study 2019. *JAMA Oncol.* 2022 Mar 1;8(3):420–444.
 11. Bray F, Laversanne M, Sung H, Ferlay J, Siegel RL, Soerjomataram I, Jemal A. Global cancer statistics 2022: GLOBOCAN estimates of incidence and mortality worldwide for 36 cancers in 185 countries. *CA Cancer J Clin.* 2024;74(3):229–63.
 12. Fan KM, Rimal J, Zhang P, Johnson NW. Stark differences in cancer epidemiological data between GLOBOCAN and GBD: Emphasis on oral cancer and wider implications. *EClinicalMedicine.* 2022;6(54): 101673.
 13. Qiu H, Cao S, Xu R. Cancer incidence, mortality, and burden in China: a time-trend analysis and comparison with the United States and United Kingdom based on the global epidemiological data released in 2020. *Cancer Commun (Lond).* 2021;41(10):1037–48.
 14. Bray F, Parkin DM; African Cancer Registry Network. Cancer in sub-Saharan Africa in 2020: a review of current estimates of the national burden, data gaps, and future needs. *Lancet Oncol.* 2022 Jun;23(6):719–728.
 15. Sung H, Ferlay J, Siegel RL, Laversanne M, Soerjomataram I, Jemal A, Bray F. Global Cancer Statistics 2020: GLOBOCAN Estimates of Incidence and Mortality Worldwide for 36 Cancers in 185 Countries. *CA Cancer J Clin.* 2021;71(3):209–49.